ELSEVIER

Journal of Organometallic Chemistry 643–644 (2002) 416–423

Journal of Organometallic Chemistry

www.elsevier.com/locate/jorganchem

Mechanism of the oxidative addition of Pd^0 complexes generated from $Pd^0(dba)_2$ and a phosphole ligand DBP: a special case where dba does not play any inhibiting role

Christian Amatore *, Anny Jutand *, Audrey Thuilliez

Département de Chimie, Ecole Normale Supérieure, UMR CNRS 8640, 24, Rue Lhomond, F-75231 Paris Cedex 5, France

Received 25 July 2001; accepted 11 September 2001

Abstract

The reactivity of the palladium(0) complexes generated from $Pd^0(dba)_2$ (dba, *trans,trans*-dibenzylideneacetone) and n equivalents 1-phenyl-dibenzophosphole (DBP) has been investigated in the oxidative addition with PhI. $Pd^0(dba)(DBP)_2$ is generated as the major complex when $n = 2$. When $n \geq 4$, the dba of $Pd^0(dba)(DBP)_2$ is substituted by the ligand to generate $Pd^0(DBP)_4$, which is the major complex in solution. Such a situation considerably differs from PPh_3, since at least 100 equivalents PPh_3 are required to completely displace dba from $Pd^0(dba)(PPh_3)_2$ to form $Pd^0(PPh_3)_3$. Consequently, dba has no decelerating effect on the kinetics of the oxidative addition of PhI to the Pd^0 complex formed from $Pd^0(dba)_2$ and n equivalents DBP ($n \geq 4$). $Pd^0(DBP)_4$ is considerably less reactive than $Pd^0(PPh_3)_4$ despite the fact that DBP is considered to be less hindered and more basic than PPh_3. $Pd^0(DBP)_2$ is the reactive species. The reaction order in the ligand DBP is -2 compared with -1 for PPh_3. The dissociation of one DBP from $Pd^0(DBP)_4$ is considerably more endergonic than that of one PPh_3 from $Pd^0(PPh_3)_4$ and is at the origin of the lower reactivity of $Pd^0(DBP)_4$. The oxidative addition of PhI generates the *trans*-$PhPdI(DBP)_2$ complex via the reversible formation of an intermediate complex assigned to *cis*-$PhPdI(DBP)_2$. © 2002 Elsevier Science B.V. All rights reserved.

Keywords: Palladium; Kinetics; Oxidative addition; Phosphole; dba

1. Introduction

The mechanism of the oxidative addition of PhI (taken as a model aryl halide) with the palladium(0) complexes generated from $Pd^0(dba)_2$ associated with n equivalents ($n \geq 2$) of monodentate phosphine ligands PPh_3 is reported in Scheme 1[1].

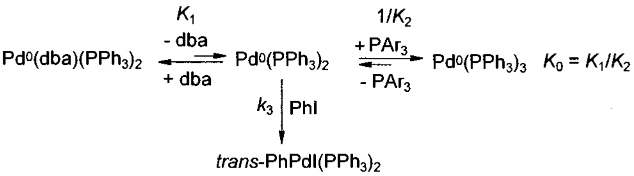

Scheme 1. Oxidative addition of PhI to the Pd^0 complex generated from $Pd^0(dba)_2$ and n equivalents PPh_3 ($n \geq 2$).

In THF or DMF, the major complex is ligated by dba: $Pd^0(dba)(PPh_3)_2$. A tris-ligated complex is formed $Pd^0(PPh_3)_3$ when $n > 2$, but $Pd^0(dba)(PPh_3)_2$ is still present. At least one hundred equivalents of PPh_3 are required to completely displace dba from $Pd^0(dba)(PPh_3)_2$. A minor complex $Pd^0(PPh_3)_2$ is the reactive species, which undergoes oxidative addition whatever $n \geq 2$. The overall reactivity is then governed by the concentration of $Pd^0(PPh_3)_2$, which is controlled by the equilibrium constants K_1 and K_2 and by the phosphine and dba concentration. Consequently, dba has a decelerating effect on the kinetics of the oxidative addition by decreasing the concentration of the active species $Pd^0(PPh_3)_2$ to form the unreactive $Pd^0(dba)(PPh_3)_2$ [1].

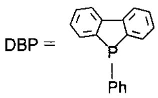

---

* Corresponding authors. Fax: + 33-1-44323325.

E-mail addresses: amatore@ens.fr (C. Amatore), anny.jutand@ens.fr (A. Jutand).

PII: S0022-328X(01)01252-9

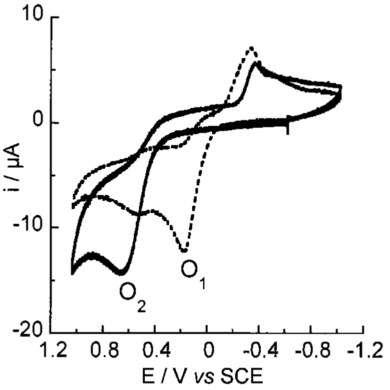

Fig. 1. Evolution with time of the cyclic voltammetry of a solution of $Pd^0(dba)_2$ (2 mmol dm^{-3}) and DBP (4 mmol dm^{-3}) in DMF (containing n-Bu_4NBF_4, 0.3 mmol dm^{-3}) at a steady gold disk electrode (2 mm diameter) with a scan rate of 0.2 V s^{-1} at 30 °C. (- - -) $t = 5$ min, O_1: oxidation of $Pd^0(DBP)_4$. (—) $t = 30$ min, O_2: oxidation of $Pd^0(dba)(DBP)_2$.

The DBP molecule [2] has been used in catalytic reactions [3]. It can be compared with PPh_3 in terms of electronic and steric properties. DBP is not planar and the phosphole ring is not aromatic [4]. DBP is considered to be more basic than PPh_3 and less bulky than PPh_3 with a smaller cone angle [5]. Consequently, $Pd^0(DBP)_2$ is expected to be intrinsically more reactive than $Pd^0(PPh_3)_2$ in oxidative additions. DBP is also less easily oxidized by dioxygen than PPh_3. It is easily synthesized [6] and is then a good candidate for industrial purposes. All these data attract our interest for this ligand even if the use of $Pd^0(dba)_2 + n$DBP as catalytic precursor is not widely developed in palladium-catalyzed reactions. We report here the mechanistic investigations on the oxidative addition of PhI to the palladium(0) complexes generated from $Pd^0(dba)_2$ associated with the phosphole ligand:DBP. Unexpectedly, the kinetic data obtained for the DBP ligand do not fit the mechanism reported in Scheme 1 and dba does not play any role in the kinetics of the oxidative addition of PhI.

2. Results and discussion

2.1. Identification of the Pd^0 complexes generated from $[Pd^0(dba)_2] + n$ equivalents DBP in DMF ($n = 2$–4)

As reported for PPh_3 [1a], the formation of Pd^0 complexes was monitored by ^{31}P-NMR spectroscopy. When two equivalents DBP were added to a solution of $Pd^0(dba)_2$ in DMF, two broad singlets ($\Delta\nu_{1/2} = 40$ Hz) of equal magnitude were observed at 17.1 and 17.5 ppm. The signal of the free ligand at -9.7 ppm was not detected. The two singlets characterize a Pd^0 complex ligated by two ligands whose phosphorous atoms are not equivalent because of the η^2 complexation of dba, as classically observed for mono or bidentate phosphine ligands [1]. $Pd^0(dba)(DBP)_2$ is then the major complex (Eq. (1)).

$$Pd^0(dba)_2 + 2DBP \rightarrow Pd^0(dba)(DBP)_2 + dba \qquad (1)$$

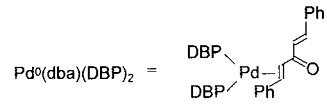

When four equivalents DBP were added to $Pd^0(dba)_2$, the two singlets of $Pd^0(dba)(DBP)_2$ were no longer observed. The free DBP signal was not observed. Only one broad signal ($\Delta\nu_{1/2} = 108$ Hz) at $\delta_1 = 10.1$ ppm was detected, which disappeared in the presence of PhI, giving rise to two new singlets at 14.3 and 22.8 ppm (vide infra). The broad signal at 10.1 ppm is then assigned to Pd^0 complexes involved in equilibrium with the ligand as classically observed [1]. In contrast to PPh_3, where the $Pd^0(dba)(PPh_3)_2$ and $Pd^0(PPh_3)_3$ coexist in solution, the dba in $Pd^0(dba)(DBP)_2$ is totally displaced by two equivalents DBP (Eqs. (2) and (3)) to form a Pd^0 complex ligated by four ligands: $Pd^0(DBP)_4$, as established from the kinetic investigation of the oxidative addition (vide infra).

$$Pd^0(dba)(DBP)_2 \overset{+2DBP}{\rightleftarrows} Pd^0(DBP)_4 + dba \qquad (2)$$

$$Pd^0(dba)_2 + 4DBP \rightleftarrows Pd^0(DBP)_4 + 2dba \qquad (3)$$

As reported for PPh_3 [1a], the formation of Pd^0 complexes from $Pd^0(dba)_2$ associated to DBP was also investigated by cyclic voltammetry, an analytical technique which allows: (i) the characterization of the $Pd^0(dba)(DBP)_2$ complex by its oxidation and reduction peaks; (ii) the characterization of $Pd^0(DBP)_4$ by its oxidation peak; and (iii) the characterization of the released dba by its two successive reduction peaks.

Addition of two equivalents of DBP to $Pd^0(dba)_2$ (2 mM) in DMF results in the formation at long times (30 min) of $Pd^0(dba)(DBP)_2$ (characterized by the oxidation wave O_2 at $+0.66$ V in Fig. 1 and a reduction wave R_2 at -1.62 V vs. SCE, not shown). This occurs via the transient formation of $Pd^0(DBP)_4$ (characterized by the oxidation wave O_1 at $+0.17$ V vs. SCE, Fig. 1), the only complex observed at short times. When $n = 4$, the oxidation peak of $Pd^0(dba)(DBP)_2$ was no longer observed and the voltammogram exhibited only the oxidation peak of $Pd^0(DBP)_4$ (wave O_1 at $+0.13$ V vs. SCE). The amount of the released dba, determined by the intensity of its reduction current at -1.62 V, increased from one to two equivalents when n varied from 2 to 4. These results confirm the NMR data but show that the formation of $Pd^0(dba)(DBP)_2$ is a complex reaction since $Pd^0(dba)(DBP)_2$ is only formed at long times (30

$$\mathrm{Pd^0(dba)_2 + 2\,DBP \xrightarrow{fast} 1/2\,Pd^0(DBP)_4 + 1/2\,Pd^0(dba)_2 + dba}$$

$$\mathrm{1/2\,Pd^0(DBP)_4 + 1/2\,Pd^0(dba)_2 \xrightarrow{slow} Pd^0(dba)(DBP)_2}$$

Scheme 2. Mechanism of the formation of $Pd^0(dba)(DBP)_2$.

min) via a disproportionation reaction involving a dba free Pd^0 complex, as already observed for bidentate ligands [1b,7] (Scheme 2).

2.2. Identification of the phenyl–Pd^{II} complexes formed in oxidative addition of PhI to the Pd^0 complexes generated from $Pd^0(dba)_2$ and n equivalents DBP in DMF ($n = 2$ or 4)

The oxidative addition of PhI (one hundred equivalents) to the Pd^0 complexes generated from $Pd^0(dba)_2$ + four equivalents DBP (Eq. (3)) was monitored by cyclic voltammetry. At short times, the oxidation peak O_1 of $Pd^0(DBP)_4$ progressively disappeared while a new oxidation peak O_3 (+0.80 V) appeared at more positive potential (Fig. 2a). As the oxidative addition proceeded, this oxidation peak O_3 disappeared and gave rise to two new oxidation peaks O_4 (+0.68 V) and O_5 (+0.43 V) (Fig. 2b). The oxidative addition proceeds then via an intermediate complex **B** oxidized at O_3, which slowly gives rise to two compounds **C** and **D** oxidized at O_4 and O_5, respectively.

The oxidative addition was also monitored by ^{31}P-NMR spectroscopy. At short times, a thin singlet was observed at $\delta_4 = 22.8$ ppm together with a broad ($\Delta\nu_{1/2} = 190$ Hz) and major signal centered at δ_3 at 14.3 ppm, which progressively disappeared to give the signals at δ_4. The singlet at δ_4 and the oxidation peak at O_4 characterize the expected complex: *trans*-PhPdI(DBP)$_2$ (**C**). This was confirmed through the result of the oxidative addition of PhI, carried out in DMF with $Pd^0(DBP)_4$, synthesized independently [8] in the absence of dba (Eq. (4)). The voltammogram exhibited a single oxidation peak at +0.68 V, similar to O_4 and the ^{31}P-NMR spectrum exhibited only one singlet at 22.8 ppm similar to δ_4 (Eq. (4)).

$$\mathrm{Pd^0(DBP)_4 + PhI \rightarrow \underset{\mathbf{C}(O_4,\,\delta_4)}{\textit{trans}\text{-}PhPdI(DBP)_2} + 2DBP} \qquad (4)$$

On the other hand, when the two ligands PPh_3 of $PhPdI(PPh_3)_2$ were exchanged by DBP (four equivalents) to form *trans*-PhPdI(DBP)$_2$ (Eq. (5)), the oxidation peak O_4 (+0.68 V) and the ^{31}P-NMR singlet at δ_4 (22.8 ppm) were also observed. Addition of dba to *trans*-PhPdI(DBP)$_2$ did not modify the voltammogram and ^{31}P-NMR spectrum.

$$\mathrm{\textit{trans}\text{-}PhPdI(PPh_3)_2 + 2DBP}$$
$$\mathrm{\rightarrow \underset{\mathbf{C}(O_4,\,\delta_4)}{\textit{trans}\text{-}PhPdI(DBP)_2} + 2PPh_3} \qquad (5)$$

The ^{31}P-NMR broad signal centered at $\delta_3 = 14.3$ ppm, which progressively disappeared to give the signal at δ_4 (*trans*-PhPdI(DBP)$_2$), was observed when the oxidative addition was performed from $Pd^0(dba)_2$ and four equivalents DBP and from the independently synthesized complex $Pd^0(DBP)_4$. The signal at δ_3 characterizes then an intermediate complex, which is formed in the very first step of the oxidative addition and may be correlated to the intermediate **B** detected by its oxidation peak O_3 (Fig. 2a). It is then assigned to the complex *cis*-PhPdI(DBP)$_2$, the primary complex formed in every oxidative addition to Pd^0 ligated by monodentate ligands (Eq. (6)) [9]. Its broad ^{31}P-NMR signal suggests that it is involved in a fast equilibrium with the starting reagents (Eq. (6)). This has been confirmed by the kinetic investigations of the oxidative addition of PhI (vide infra).

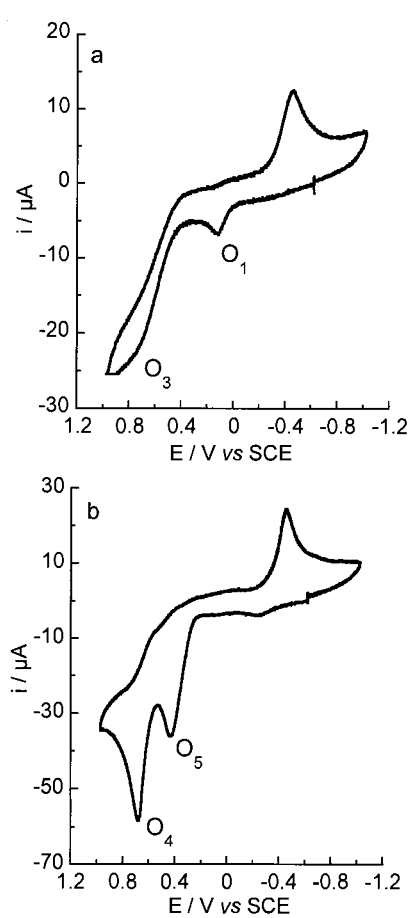

Fig. 2. Oxidative addition of PhI (200 mmol dm^{-3}) to the Pd^0 complex generated from $Pd^0(dba)_2$ (2 mmol dm^{-3}) and DBP (8 mmol dm^{-3}) in DMF (containing *n*-Bu$_4$NBF$_4$, 0.3 mmol dm^{-3}) monitored by cyclic voltammetry at a steady platinum disk electrode (2 mm diameter) with a scan rate of 0.2 V s^{-1} at 30 °C. (a) $t = 6$ min, O_1: oxidation of $Pd^0(DBP)_4$, O_3: oxidation of the intermediate complex *cis*-PhPdI(DBP)$_2$ early formed in the oxidative addition. (b) $t = 130$ min, O_4: oxidation of *trans*-PhPdI(DBP)$_2$, O_5: oxidation of I$^-$.

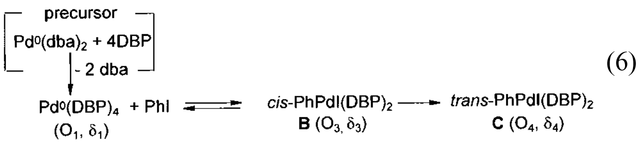

(6)

The half-life time of the intermediate **B** was higher when the oxidative addition was monitored by ^{31}P-NMR spectroscopy than when the reaction was monitored by cyclic voltammetry. This reflects a concentration effect since a main difference between the two reactions was the reagents concentration, ^{31}P-NMR spectroscopy requiring higher concentrations, ten times higher for each reagent: Pd(dba)$_2$, DBP and PhI.

At longer times, a new minor thin singlet appeared at $\delta_5 = 14.3$ ppm, which is correlated to the unknown oxidation peak at O$_5$ (Fig. 2b). This compound **D** was formed by decomposition of the *trans*-PhPdI(DBP)$_2$ complex. The oxidation peak at O$_5$ characterizes I$^-$ ions as evidenced by the increase of its current intensity upon addition of n-Bu$_4$NI. Consequently, the thin singlet at $\delta_5 = 14.3$ ppm characterizes a compound **D** which contains one or two equivalents P atoms associated to I$^-$ ions, i.e. a ionic species. Since **D** was not formed in the fast reaction where *trans*-PhPdI(DBP)$_2$ was generated from *trans*-PhPdI(PPh$_3$)$_2$ by ligand exchange (Eq. (5)), **D** cannot be the cationic complex *trans*-PhPdS(DBP)$_2^+$, I$^-$ (S, solvent), which could have been generated by dissociation of the neutral *trans*-PhPdI(DBP)$_2$ complex, as observed for *trans*-PhPdI(PPh$_3$)$_2$ [10]. **D** could have been a phosphonium salt [DBP–Ph]$^+$I$^-$, which might have been formed at long times by a reductive elimination [11] in *trans*-PhPdI(DBP)$_2$. The phosphonium salt [DBP–Ph]$^+$BF$_4^-$ was synthesized independently by reacting DBP and the diazonium salt PhN$_2^+$BF$_4^-$. Its ^{31}P-NMR signal was not located at 14.3 ppm but at 22.8 ppm. The formation of PdI$_2$(DBP)$_2$ [12] was also ruled out since its ^{31}P-NMR signal is located at 4.7 ppm.

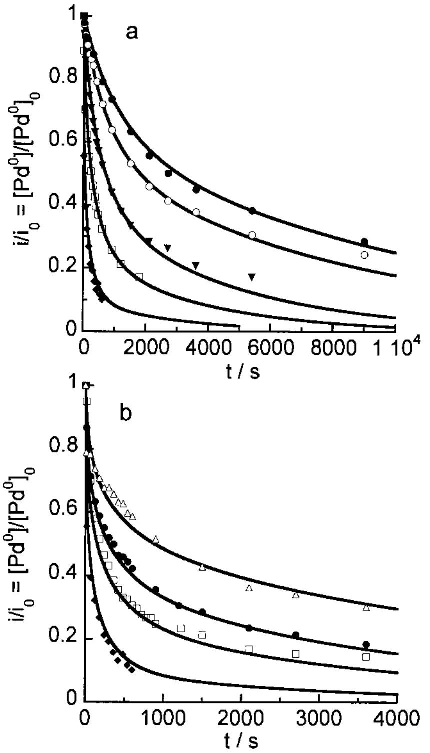

Fig. 3. Kinetics of the oxidative addition of PhI to the Pd^0 complex generated from Pd^0(dba)$_2$ (2 mmol dm^{-3}) and n equivalents DBP in DMF (containing n-Bu$_4$NBF$_4$, 0.3 mmol dm^{-3}) monitored by cyclic voltammetry at a steady platinum disk electrode (2 mm diameter) with a scan rate of 0.2 V s^{-1}, at 30 °C. Plot of $i/i_0 = [\mathrm{Pd}^0]/[\mathrm{Pd}^0]_0$ versus time (i: oxidation current of peak O$_1$ at t, i_0: initial oxidation current of peak O$_1$). (a) Influence of the DBP concentration for [PhI] = 200 mmol dm^{-3}: [DBP] = (◆) 8; (□) 10; (▼) 12; (○) 14; (●) 16 mmol dm^{-3}. (b) Influence of the PhI concentration for [DBP] = 8 mmol dm^{-3}: [PhI] = (◆) 200; (□) 80; (●) 40; (△) 20 mmol dm^{-3}. The solid lines are the theoretical kinetic curves simulated according to the mechanism of Scheme 3.

At this level of our investigation, the overall oxidative addition when performed from Pd^0(dba)$_2$ precursor associated with four equivalents DBP can be schematically described by Eq. (6). An unknown compound **D** is formed at long times.

When the oxidative addition of PhI was performed from Pd^0(dba)$_2$ + two equivalents DBP, i.e. from Pd^0(dba)(DBP)$_2$ (Eq. (1)), the ^{31}P-NMR spectrum also exhibited at the end of the oxidative addition the two thin singlets (δ_4 and δ_5) of *trans*-PhPdI(DBP)$_2$ and **D**, respectively.

2.3. Identification of the reactive Pd^0 complex generated from Pd^0(dba)$_2$ + n equivalents DBP in DMF ($n \geq 4$)

The oxidative addition of PhI to the Pd^0 complexes formed from Pd^0(dba)$_2$ + two equivalents DBP, could not be monitored by amperometry, as usually done in our group [1], since: (i) the oxidation peaks of Pd^0(dba)(DBP)$_2$ at O$_2$ (+0.66 V) and *trans*-PhPdI(DBP)$_2$ at O$_4$ (+0.68 V) are too close and (ii) the I$^-$ ions also formed in this reaction are oxidized at O$_5$ (+0.47 V), i.e. at less positive potential than the oxidation potential of Pd^0(dba)(DBP)$_2$ at O$_2$ (+0.66 V). Consequently, due to the vicinity of the oxidation peaks of the starting and final complexes, the kinetics of the oxidative addition of PhI to Pd^0(dba)(DBP)$_2$ formed from Pd^0(dba)$_2$ + two equivalents DBP could not be monitored by amperometry at a rotating disk electrode. The kinetics was then investigated from mixtures containing larger amounts of DBP ($n \geq 4$) so that the complex Pd^0(dba)(DBP)$_2$ was not formed and the major complex was dba-free Pd^0 complex(es) Pd^0(DBP)$_{n'}$ (with $n' = 3$ or 4) oxidized at less positive potential (O$_1$ at +0.17 V). The oxidative addition was then monitored by performing cyclic voltammetry at a steady electrode as a function of time and by plotting the variation of the intensity of the oxidation peak current of $Pd^0(DBP)_{n'}$ (proportional to the Pd^0 concentration) versus time (Fig. 3a–b). This avoided any overlapping of the oxidation current of the Pd^0 complex(es) with that of the I^- ions. When considering the DBP ligand, one observes in Fig. 3a–b that the decay of the Pd^0 concentration does not obey an exponential law. The kinetics proceeds in two successive steps, the first one being faster than the second one. This suggests the reversible formation of an intermediate complex **B** (vide supra), which accumulates and then slowly gives the final complex **C** (Eq. (7)).

$$\mathbf{A} \rightleftarrows \mathbf{B} \rightarrow \mathbf{C} \qquad (7)$$

Therefore, the mechanism of the oxidative addition seems to be more complex for DBP than for PPh_3, for which whatever the experimental conditions, the decay of the Pd^0 concentration always obeys a classical exponential law with a reaction order in PhI of + 1 and − 1 for dba and PPh_3 (Scheme 1).

2.3.1. Influence of the dba concentration

When $n = 4$, we have seen above that $Pd^0(dba)(DBP)_2$ was not formed in appreciable concentration. The only complex(es) in solution were free dba Pd^0 complex(es) $Pd^0(DBP)_{n'}$ ($n' = 3$ or 4). However, $Pd^0(dba)(DBP)_2$ could exist at traces level and be involved in an equilibrium with the expected reactive species $Pd^0(DBP)_2$ (Eq. (8)).

$$Pd^0(dba)(DBP)_2 \rightleftarrows Pd^0(DBP)_2 + dba \qquad (8)$$

In such a situation, in the presence of added dba, the equilibrium (Eq. (8)) is expected to be shifted towards the formation of $Pd^0(dba)(DBP)_2$. The concentration of the reactive species $Pd^0(DBP)_2$ should decrease and the kinetics should be slowed down. But the oxidative addition was not affected by the dba concentration (Fig. 4). This implies that in the presence of four equivalents DBP, the equilibrium (Eq. (8)) is not easily shifted towards $Pd^0(dba)(DBP)_2$ by dba. dba is then a less good ligand for $Pd^0(DBP)_2$ than for $Pd^0(PPh_3)_2$. Consequently, when $n \geq 4$, we can consider that the equilibrium (Eq. (8)) does not interfere in the kinetics of the oxidative addition. Only dba free complexes $Pd^0(DBP)_{n'}$ are involved in the oxidative addition ($n' =$ 2, 3, 4).

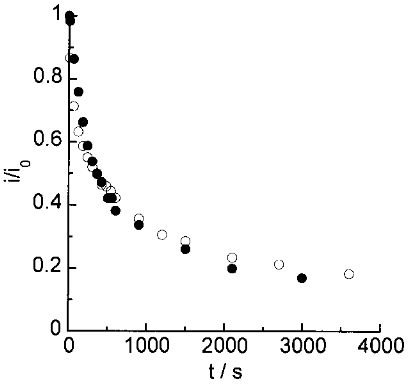

Fig. 4. Kinetics of the oxidative addition of PhI (200 mmol dm^{-3}) to the Pd^0 complex generated from $Pd^0(dba)_2$ (2 mmol dm^{-3}) and DBP (8 mmol dm^{-3}) in DMF (containing n-Bu_4NBF_4, 0.3 mmol dm^{-3}) monitored by cyclic voltammetry at a steady platinum disk electrode (2 mm diameter) with a scan rate of 0.2 V s^{-1}, at 30 °C. Plot of $i/i_0 = [Pd^0]/[Pd^0]_0$ versus time (i: oxidation current intensity of peak O_1 at t, i_0: initial oxidation current intensity of peak O_1). Influence of the added dba concentration: [dba] = (○) 0; (●) 100 mmol dm^{-3}.

2.3.2. Influence of the DBP concentration

The oxidative addition of PhI (one hundred equivalents) was considerably slowed down by addition of DBP: n in the range 4–8 (Fig. 3a). This implies that the reactive Pd^0 species is involved in an equilibrium with DBP and more ligated Pd^0 complex(es). The half-reaction time of the oxidative addition did not increase linearly with the concentration of DBP, which excludes a reaction order of − 1 for DBP. The high decelerating effect observed in the presence of excess DBP suggests a reaction order higher than − 1 for the ligand with a mechanism involving successive reversible decomplexations of DBP from the complex $Pd^0(DBP)_{n'}$ generated from $Pd(dba)_2$ and n equivalents DBP (Scheme 3, Eq. (9)).

As seen in Fig. 3a, due to the large decelerating effect of the ligand DBP, only low excesses of DBP were investigated (from four to eight equivalents per $Pd(dba)_2$) even in the presence of PhI in large excess (100 equivalents). Since DBP is continuously released in equilibrium (Eq. (9)) when the oxidative reaction proceeds, the concentration of DBP cannot be considered as being constant during the reaction, which results in very complex kinetic laws. This is why only the kinetic data obtained at short times were considered, i.e. when the concentration of DBP did not vary too much. At short times, the reactions involving the evolution of **B**, i.e. those with the rate constants k_{-2} and k_3 may be neglected (Scheme 3). The initial rate V_0 is then expressed as in Eq. (11) (L = DBP). [L] is the free ligand

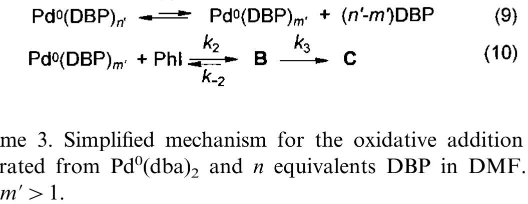

Scheme 3. Simplified mechanism for the oxidative addition of PhI generated from $Pd^0(dba)_2$ and n equivalents DBP in DMF. $n' \leq 4$; $n' - m' > 1$.

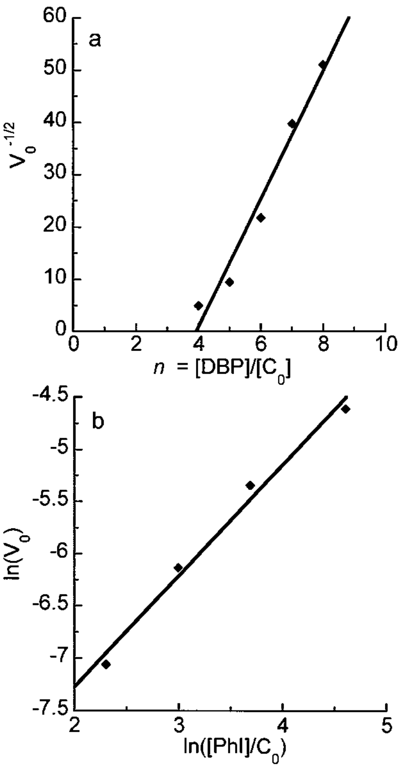

Fig. 5. Oxidative addition of PhI to the Pd^0 complex generated from $Pd^0(dba)_2$ ($C_0 = 2$ mmol dm^{-3}) and n equivalents DBP in DMF at 30 °C. (a) Determination of the reaction order in DBP: variation of $V_0^{-1/2}$ (V_0: initial slope of the kinetic curves of Fig. 3a) vs. n ($n = [DBP]/C_0$) (see Eq. (12) with $n' - m' = 2$). (b) Determination of the reaction order in PhI: variation of ln V_0 (V_0: initial slopes of the kinetic curves of Fig. 3b) vs. ln([PhI]/C_0).

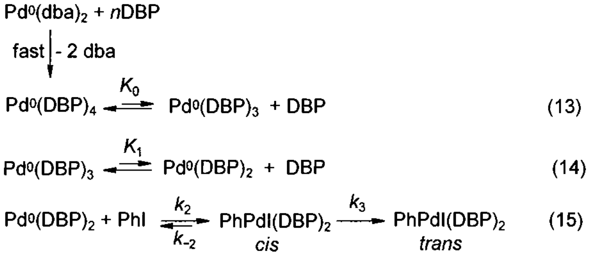

Scheme 4. Mechanism of the oxidative addition of PhI to $Pd^0(DBP)_4$ generated from $Pd^0(dba)_2$ and n equivalents DBP ($n \geq 4$) in DMF.

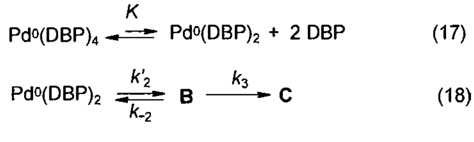

Scheme 5. Simplified mechanism for the oxidative addition.

concentration at $t = 0$: $[L] = (n - n')C_0$ where C_0 is the initial concentration of $Pd(dba)_2$.

$$V_0 = d[Pd^0L_4]/dt = Kk_2[PhI][Pd^0L_{n'}]/[L]^{(n'-m')} \qquad (11)$$

Eq. (12) is the simplified expression of Eq. (11).

$$V_0^{-1/(n'-m')} = A(n - n') \qquad (12)$$

The plot of $V_0^{-1/2}$ (V_0: initial slope of the kinetic curves of Fig. 3a) versus n is a straight line (Fig. 5a). This shows that $n' - m' = 2$ (Eq. (12)) and the reaction order in DBP is then -2. The value of $V_0^{-1/2}$ is zero when $n = 4$ (Fig. 5a), which shows that $n' = 4$ (Eq. (12)).

Consequently, the major Pd^0 complex formed from $Pd(dba)_2$ and n equivalents DBP ($n \geq 4$) is $Pd^0(DBP)_4$ (Scheme 4). $Pd^0(DBP)_2$ is the reactive species, which is formed after two successive reversible decomplexations of the ligand from $Pd^0(DBP)_4$ with, in the first one, $K_0/[DBP] \ll 1$ (Scheme 4, Eq. (13)). This situation quite differs from that of PPh_3. In that case, the reaction order is -1 for PPh_3 [13] because the first decomplexation from $Pd^0(PPh_3)_4$ to form $Pd^0(PPh_3)_3$ is almost irreversible ($K_0/[PPh_3] \gg 1$), so that the major complex in solution is $Pd^0(PPh_3)_3$ and the oxidative addition proceeds then from $Pd^0(PPh_3)_2$ after decomplexation of one phosphine [13]. This is the reason why $Pd^0(DBP)_4$ is considerably less reactive with PhI than $Pd^0(PPh_3)_4$ [1a], by a factor 500.

2.3.3. *Influence of the PhI concentration*

The rate of the oxidative addition of PhI increased with the PhI concentration (Fig. 3b). At short times, the reactions with the rate constants k_{-2} and k_3 may be neglected (Scheme 4) and the expression of the initial rate V_0 is given by Eq. (16).

$$V_0 = K_0K_1k_2[PhI][Pd^0L_4]/[L]^2 \qquad (16)$$

The plot of $\ln(V_0)$ (V_0, initial slope of the kinetic curves of Fig. 3b) versus ln[PhI] is a straight line (Fig. 5b) with a slope of $+1$, which confirms the reaction order of $+1$ in PhI, as postulated in Scheme 4. The value of $K_0K_1k_2 = 6.7 \times 10^{-5}$ M s^{-1} (at 30 °C) is calculated from the slope of the regression line of Fig. 5a.

The theoretical kinetic curves have been simulated using numerical finite differences (C ANSI language) on the basis of the simplified mechanism in Scheme 5 (k'_2 is an apparent rate constant: $k'_2 = k_2[PhI]$).

The theoretical curves fit the experimental data (Fig. 3a,b). From the simulations, it is possible to determine a set of values for k_{-2}, k_3 and Kk'_2 for different PhI concentrations, which were plotted versus PhI concentration (Fig. 6). k_{-2} and k_3 did not vary with PhI concentration whereas Kk'_2 varied linearly with PhI concentration. $Kk'_2 = K_0K_1k_2[PhI]$. These results validate the mechanism of Scheme 4. The rate constants have been calculated from these sets of values:

$k_{-2} = 1.8 \times 10^{-4}$ s^{-1}; $k_3 = 4.5 \times 10^{-4}$ s^{-1};

$K_0K_1k_2 = 7.7 \times 10^{-5}$ M s^{-1} in DMF at 30 °C

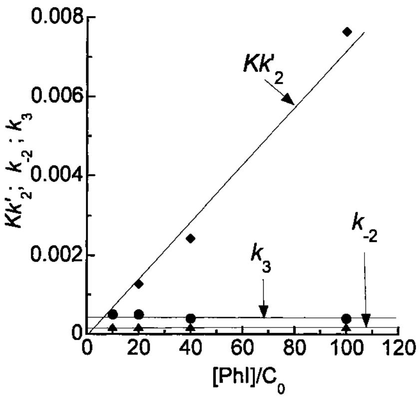

Fig. 6. Oxidative addition of PhI to the Pd^0 complex generated from $Pd^0(dba)_2$ ($C_0 = 2$ mmol dm^{-3}) and four equivalents DBP in DMF. Plot of Kk'_2, k_{-2} and k_3 (determined from the simulated theoretical curves of Fig. 3b, Scheme 4) vs. PhI concentration.

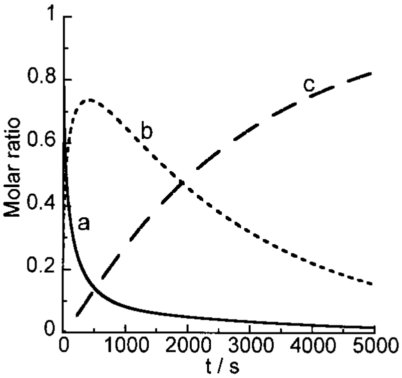

Fig. 7. Theoretical curves for the oxidative addition of PhI (200 mmol dm^{-3}) to the Pd^0 complex generated from $Pd^0(dba)_2$ (2 mmol dm^{-3}) and four equivalents DBP. (a) Molar ratio of $Pd^0(DBP)_4$ vs. time. (b) Molar ratio of the intermediate complex assigned to *cis*-$PhPdI(DBP)_2$ vs. time. (c) Molar ratio of *trans*-$PhPdI(DBP)_2$ vs. time. Curve *b* is determined from curves *a* and *c*: $b = 1 - (a + c)$.

The latter value is very close to that estimated from the initial rate (6.7×10^{-5} M s^{-1}, vide supra). Using these rate constants values, the kinetics of the formation of the compound **C** has been simulated (Fig. 7, curve c), as well as the kinetics of the formation of the intermediate compound **B** (Fig. 7, curve *b*, $b = 1 - (a + c)$). When $[Pd(dba)_2] = 2$ mM, $[DBP] = 8$ mM and $[PhI] = 0.2$ M, the concentration of **B** is maximum for a reaction time of 400 s, which corresponds to the life time observed for the species oxidized at O_3 (Fig. 2b), i.e. when the oxidative addition was performed under the same experimental conditions and monitored by cyclic voltammetry. This justifies a posteriori the mechanism proposed in Scheme 4.

3. Conclusion

Whereas dba has a decelerating effect on the kinetics of the oxidative addition of PhI to $Pd^0(dba)_2$ and *n* equivalents PPh_3 ($n \geq 2$), the situation is quite different when considering the DBP ligand. Indeed, as soon as $n = 4$, dba does not play any role in the kinetics of the oxidative addition since the major Pd^0 complex is $Pd^0(DBP)_4$. $Pd^0(DBP)_4$ is considerably less reactive than $Pd^0(PPh_3)_4$ [1a] (by a factor 500) despite the fact that DBP is considered to be less hindered and more basic than PPh_3, two factors which are in favor of faster oxidative additions. The reactive species is $Pd^0(DBP)_2$ and the reaction order in DBP is -2 compared with -1 for PPh_3. The lower reactivity of $Pd^0(DBP)_4$ compared with that of $Pd^0(PPh_3)_4$ is due to the fact that the dissociation of one DBP from $Pd^0(DBP)_4$ is considerably more endergonic than that of one PPh_3 from $Pd^0(PPh_3)_4$ and is responsible for the reaction order in DBP of -2. The concentration of the reactive $Pd^0(DBP)_2$ generated from $Pd^0(DBP)_4$ is then considerably lower than that of $Pd^0(PPh_3)_2$ generated from $Pd^0(PPh_3)_4$. This counterbalances the expected higher intrinsic reactivity of $Pd^0(DBP)_2$ compared with that of $Pd^0(DBP)_2$. $Pd^0(DBP)_4$ is more stable in solution than $Pd^0(PPh_3)_4$ because DBP is a less hindered ligand, which induces less steric constraints around the Pd^0 center.

The oxidative addition of PhI generates the expected *trans*-$PhPdI(DBP)_2$ via the reversible formation of an intermediate complex whose half-reaction time allows its detection in cyclic voltammetry and ^{31}P-NMR spectroscopy. This intermediate complex is assigned to *cis*-$PhPdI(DBP)_2$.

4. Experimental

4.1. General

^{31}P-NMR spectra were recorded on a Bruker spectrometer (101 MHz) using H_3PO_4 as an external reference. Cyclic voltammetry was performed with a home made potentiostat and a wave form generator Tacussel GSTP4. The cyclic voltammograms were recorded on a Nicolet oscilloscope (310).

4.2. Chemicals

DMF was distilled from calcium hydride under vacuum and kept under argon. Commercial phenyl iodide (Acros) was used after filtration on alumina. The DBP ligand was commercial (Strem). $Pd(dba)_2$ was synthesized from a reported procedure [14] but starting from Na_2PdCl_4 instead of $PdCl_2$. $Pd^0(DBP)_4$ [8] and $PhPdI(PPh_3)_2$ [15] were prepared according to described procedures.

4.3. Cyclic voltammetry experiments

Electrochemical experiments were carried out in a three electrode cell connected to a Schlenk line. The cell was equipped with a double envelope to maintain a constant temperature of 30 °C (Lauda RC20 thermostat). The working electrode was steady a gold disk of 2 mm diameter. The counter electrode was a platinum wire of ca. 1 cm^2 apparent surface area. The reference was a saturated calomel electrode separated from the solution by a bridge filled with a solution of n-Bu_4NBF_4 (0.3 mol dm^{-3}) in three milliliters of DMF. Fifteen milliliters of DMF containing the same concentration of supporting electrolyte was poured into the cell. Seventeen milligrams of $Pd(dba)_2$ (0.03 mmol) was then added, followed by the suitable amount of the DBP ligand. The cyclic voltammetry was performed at a scan rate of 0.2 V s^{-1}. The kinetic measurements were performed at 30 °C under the same experimental conditions, using a steady platinum disk of 2 mm diameter as the working electrode. The suitable amount of phenyl iodide was added and the cyclic voltammetry was performed at a scan rate of 0.2 V s^{-1} as a function of time to monitor the kinetics of the oxidative addition.

Acknowledgements

This work has been supported by the Centre National de la Recherche Scientifique (CNRS, UMR 8640) and the Ministère de la Recherche (Ecole Normale Supérieure).

References

[1] (a) C. Amatore, A. Jutand, F. Khalil, M.A. M'Barki, L. Mottier, Organometallics 12 (1993) 3168;
(b) C. Amatore, A. Jutand, Coord. Chem. Rev. 178–180 (1998) 511.

[2] G. Wittig, G. Geissler, Ann. Chem. 580 (1953) 44.

[3] (a) A. Sisak, F. Ungvary, G. Kiss, J. Mol. Catal. 18 (1983) 223;
(b) D.G. Holah, A.N. Hughes, B.C. Hui, Can. J. Chem. 50 (1972) 3714;
(c) D. Budd, D.G. Holah, A.N. Hughes, B.C. Hui, Can. J. Chem. 52 (1974) 775;
(d) L.M. Wilkes, J.H. Nelson, L.B. McCusker, K. Seff, F. Mathey, Inorg. Chem. 22 (1983) 2476;
(e) R. Vac, J.H. Nelson, E.B. Milosavljevic, L. Solujic, Inorg. Chem. 28 (1989) 3831;
(f) W.A. Herrmann, C. Brossmer, K. Öfele, M. Beller, H. Fisher, J. Mol. Catal. A 103 (1995) 133;
(g) T. Hayashi, M. Tanka, I. Ogata, J. Mol. Catal. 6 (1979) 1.

[4] W. Egan, R. Tang, G. Zon, K. Miskow, J. Am. Chem. Soc. 17 (1971) 6205.

[5] D.W. Allen, D. Hogarth, Phosphorus Sulfur 3 (1977) 381.

[6] H. Hoffmann, Chem. Ber. 95 (1962) 2563.

[7] C. Amatore, G. Broeker, A. Jutand, F. Khalil, J. Am. Chem. Soc. 119 (1997) 5176.

[8] D.T. Rosevear, F.G.A. Stone, J. Chem. Soc. A (1968) 164.

[9] (a) H. Urata, M. Tanaka, T. Fuchikami, Chem. Lett. (1987) 751;
(b) A.L. Casado, P. Espinet, Organometallics 17 (1998) 954.

[10] C. Amatore, E. Carré, A. Jutand, Acta Chem. Scand. 52 (1998) 76.

[11] (a) F.E. Goodson, T.I. Wallow, B.M. Novak, J. Am. Chem. Soc. 119 (1997) 12441;
(b) F.Y. Kwong, K.S. Chan, Chem. Commun. (2000) 1069.

[12] $PdI_2(DBP)_2$ was synthesized as for $PdI_2(PPh_3)_2$. See: C. Amatore, M. Azzabi, A. Jutand, J. Am. Chem. Soc. 113 (1991) 8375.

[13] J.F. Fauvarque, F. Pflüger, M. Troupel, J. Organomet. Chem. 208 (1981) 419.

[14] Y. Takahashi, T. Ito, S. Sakai, Y. Ishii, J. Chem. Soc. Chem. Commun. (1970) 1065.

[15] P. Fitton, E.A. Rick, J. Organomet. Chem. 28 (1971) 287.